PCCP

PAPER

View Article Online
View Journal | View Issue

Cite this: *Phys. Chem. Chem. Phys.*, 2019, **21**, 6178

Tuning of the gold work function by carborane films studied using density functional theory†

Martin Hladík, Aliaksei Vetushka, Antonín Fejfar* and Héctor Vázquez *

Received 18th January 2019,
Accepted 20th February 2019

DOI: 10.1039/c9cp00346k

rsc.li/pccp

Using density functional theory including van der Waals interactions, we calculate the adsorption and electronic properties of dithiol-dicarba-*closo*-dodecaboranes chemisorbed on Au(111) surfaces. Carborane molecules consist of a cage-like structure made of boron and carbon atoms and possess a large intrinsic dipole. We consider two functionalized carborane positional isomers, with thiol linker groups attached to either carbon or boron backbone atoms, such that when adsorbed on the Au substrate, the molecular dipole points towards the metal surface or away from it. We investigate a large number of junction geometries and find that carborane adsorption can induce significant changes in the work function of the Au substrate, in the range of 1 eV. These changes depend strongly on the interface geometry at the atomistic level. From the analysis of these junction structures, we provide a picture of the driving mechanisms that determine adsorption geometries, and relate them to interface electronic structure and resulting work function modification. In particular, our results highlight the important role played in these interface quantities by distortions in the Au surface layer induced by carborane adsorption.

1 Introduction

Self-assembled monolayers (SAMs), a large set of molecules creating two-dimensional (2D) interfaces most commonly between gaseous and solid phases, enable the tuning of surface properties suitable for use in materials development and nanotechnology.[1,2] Changes in the surface properties can ultimately lead to increased efficiency of photovoltaic cell efficiency through the tuning of molecular level positions of SAMs composed of electronically active molecules.[3–6]

Rigid molecules with a cage-like structure have attracted attention among SAMs due to their higher stability against heating and chemical substitution and small number of defects of formed monolayers.[7–11] Dicarba-*closo*-dodecaboranes (commonly known as carboranes) are particularly attractive given their remarkable electronic structure properties (Fig. 1).[12–15] In coordination chemistry, carboranes are employed as suitable ligands for transition-element complexes,[16–19] or as part of polymer materials.[20] When functionalized with thiol linker groups,[3,21–29] carboranethiols have been used as building blocks for SAMs on metal surfaces,[1,25,26,30,31] even tuning the binding configuration to the substrate.[32]

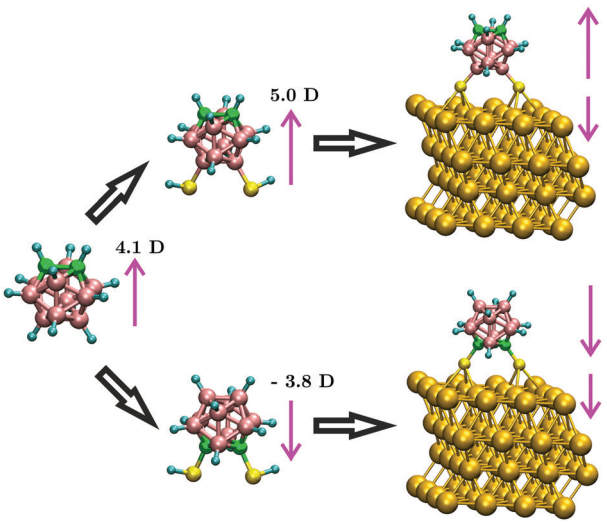

Fig. 1 Isolated carborane molecules and adsorption of dithiol-*ortho*-carboranes on Au(111). The large molecular dipole originates from an asymmetry in the electron density caused by the position of carbon and boron atoms in the cage.

The remarkable electronic properties of carboranes and carboranethiols are closely related to their significant molecular dipole. The carborane molecule ($C_2B_{10}H_{12}$) has an icosahedral geometry with 20 sides and 12 vertices, in which the 2 carbon and 10 boron atoms are hexacoordinated and participating in the heavily delocalized bonds.[16,17] The different electronegativity

Institute of Physics, Academy of Sciences of the Czech Republic, Cukrovarnická 10, 162 00 Prague, Czech Republic. E-mail: fejfar@fzu.cz, vazquez@fzu.cz

† Electronic supplementary information (ESI) available: Metal–molecule structures for geometry optimization calculations; convergence of geometry and electronic structure with k-point sampling; STM images; effect of Au surface asperity: adatom and trimer structures. See DOI: 10.1039/c9cp00346k

of C and B atoms results in a non-uniform electron density distribution, which, depending on the position of C and B atoms, can lead to substantial molecular dipoles. In this paper we consider 1,2-dicarba-*closo*-dodecaboranes (commonly known as *ortho*-carboranes, Fig. 1, left), which is the isomer with the largest molecular dipole.[16,17] Dithiol functionalization of *ortho*-carboranes can be done at the C atoms or at the B atoms, which further modifies the molecular dipole (Fig. 1, middle). When adsorbed on a metal surface, the details of interface geometry and binding are known to play a role.[16,17,33] As we show in this paper, metal–molecule hybridization and resulting charge transfer and rearrangement strongly affect the interface electronic structure, allowing us to change the work function of the metal surface by more than 1 eV.

2 Computational details

Dithiol *ortho*-carborane molecules were adsorbed on an Au(111) surface (with the H atoms of the thiol linker groups removed). Geometry relaxations were carried out using density functional theory for a large number of structures. Calculations were done using the SIESTA[34] code. A local-orbital single-ζ plus polarization basis was used for gold atoms, while molecular atoms were described with a double-ζ plus polarization basis. The largest (shell-dependent) values for the radial confinement radii used in our calculations are (Bohr): 6.459 (boron), 5.205 (hydrogen), 5.519 (carbon), 5.487 (sulfur), 6.723 and 10.544 (gold). The larger cutoff radii for surface layer Au atoms and adatoms provide a better description of the wave function decay into the vacuum. Exchange–correlation, including van der Waals interactions, was described using the vdW-DF functional of M. Dion *et al.*[35] in the implementation of G. Román-Pérez and J. M. Soler.[36] The unit cell contained the molecule plus 4 Au layers, each of which consisted of 16 atoms. With this lateral size, the effect of unit cell replicas on molecular geometry was small. This was checked by optimizing the geometry in larger unit cells (36 atoms per layer and equivalent Brillouin zone sampling). Going from the 16- to the 36-atom-per-layer cell (areas of 122 and 275 Å^2 respectively), the position of each carborane atom changed by only 0.004 Å on average. A vacuum gap of $\sim$10 Å was introduced above the topmost molecular atom. Slab dipole corrections were taken into account. The position of molecular and Au surface layer atoms was relaxed until residual forces fell below 0.02 eV Å^{-1}. A 250 Ry real-space cutoff was used in the calculations. Reciprocal space in the direction parallel to the surface was sampled with a 6 $\times$ 6 Monkhorst–Pack grid for geometry relaxations and for the calculation of electron density and electrostatic potential energy, which we checked were sufficiently converged.

3 Results

Geometries

We systematically investigated a large number of interface structures by probing the azimuthal angle with respect to Au rows as well as the molecular tilt angle. We generated initial geometries for optimization by placing the center of the carborane cage above a Au–Au bond. We changed the azimuthal angle (defined by the line connecting both S atoms with the row of surface Au atoms) in steps of 10 degrees between 0 and 120 degrees. Each of these initial structures was relaxed. Simulations showed that metal–molecule junction structure was driven by the binding of the S atoms and influenced by the molecular tilt angle. Final geometries consistently showed S atoms adsorbed near hollow sites on the Au surface. In these positions, azimuthal angles are close to either 10 or 110 degrees (equivalent by symmetry).

To investigate the role played by the polar angle, each of these final geometries was then tilted around the S–S bond an angle ranging from 0 to 70 degrees (in steps of 10 degrees), and the geometry was optimized again.

Thus over a hundred structures with different initial azimuthal and polar angles were explored, each of which resulted in a local minimum. This was done for both B- and C-bonded isomers.

Work function change

We first discuss the work function changes resulting from carborane adsorption by analyzing the changes for B- and C-bonded molecules adsorbed vertically. Fig. 2 shows the calculated

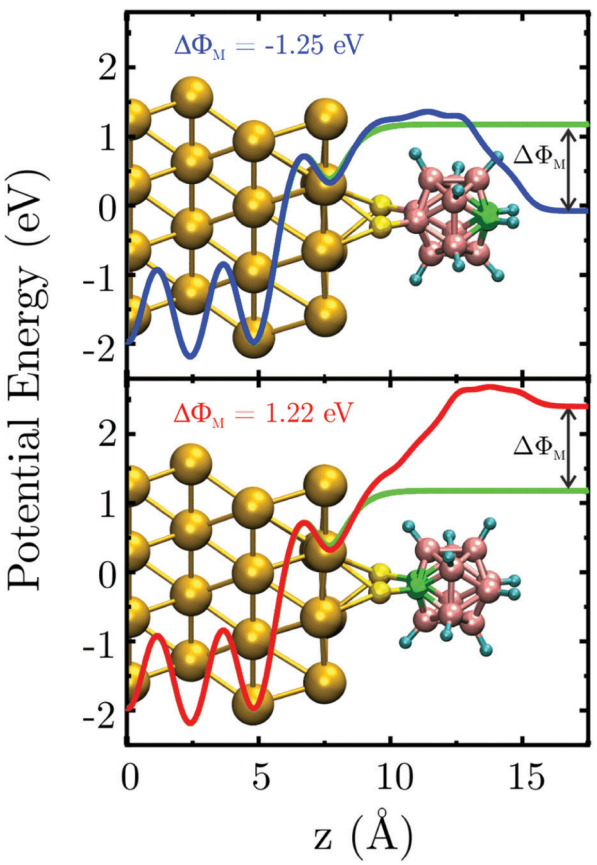

Fig. 2 Plane-averaged potential energy profiles for B-bonded (top) and C-bonded (bottom) carboranethiols adsorbed on Au(111). Green curves correspond to the clean Au(111) slab.

plane-averaged electrostatic potential across the junctions[37–40] as a function of the distance to Au reference layers.

The figure shows the potential for the B-bonded conformer (top panel, blue line) and for the C-functionalized conformer (bottom panel, red line). The figure also shows the potential for the clean Au(111) surface (green line), which is the same in both panels.

Three main regions can be clearly distinguished as a function of distance to the surface. Up to $z \sim 5$ Å, oscillations in the electrostatic potential are regular and the behavior is bulk-like. Then there is an intermediate region (extending between $\sim$7 and $\sim$10 Å for the clean surface and between $\sim$7 and $\sim$15 Å for the carborane junctions) with significant variations resulting from surface and interface effects; their origin is discussed in detail in the following section. Finally, beyond $\sim$15 Å the potential is flat. Importantly, the height of this outer flat plateau, which characterizes the work function of the metal–molecule interface, is different from the clean surface and among both carborane terminations. Deep inside the metal the electronic structure is not affected by surface or interface effects, and all three profiles match. In the interface region, differences start to appear between the carborane-terminated junctions and the clean surface, as well as between both carborane systems. Far from the junction, the three potential profiles level out to different values, illustrating the effect of the carborane layers on the work function. Depending on which chemical species in the cage-like backbone the S linkers are attached to, the potential profile (reflecting the value of the work function) can be shifted by $\sim$1 eV in either direction compared to the clean surface.

For B-bonded carborane, the work function is reduced by 1.25 eV, while for the C-functionalized isomer, it is increased by 1.22 eV. The results of Fig. 2 show that the range of possible metal surface work function shifts upon carborane adsorption on the clean Au(111) is about 2.5 eV. This trend in work function changes is consistent with results of Kelvin Probe Force Microscopy experiments of carboranes measured previously.[41,42]

The sign of the work function modification can be understood from the direction of the molecular dipole of the thiol-terminated carborane. The calculated dipole along the z direction of the clean Au surface is -4.4 D, while that of the B-bonded (C-bonded) molecule with the H atoms from the thiol linkers removed is +6.1 D (-1.7 D). The sign of these unit cell dipoles indicates their orientation, from negative to positive charge, along the z axis.

Electron density difference

To characterize the details of interface electronic structure, we investigate the charge rearrangement upon carborane adsorption, given by the plane-averaged electron density difference $\rho_{\mathrm{diff}}(z)$. This quantity is defined as the difference between the electron density of the metal–molecule junction $\rho_{\mathrm{jcn}}(z)$ and the sum of electron densities of the isolated molecule $\rho_{\mathrm{mol}}(z)$ and metal surface $\rho_{\mathrm{Au}}(z)$:

$$\rho_{\mathrm{diff}}(z) = \rho_{\mathrm{jcn}}(z) - [\rho_{\mathrm{mol}}(z) + \rho_{\mathrm{Au}}(z)] \quad (1)$$

When calculating these quantities, geometry was kept frozen so as to compute only electronic effects. All densities in eqn (1) are averaged over the x and y components in the unit cell.[39,43,44] In the calculation of ρ_{mol}, the H atoms in the thiol groups are not included.

Fig. 3 shows the calculated electron density difference for the B- and C-bonded carboranes. Positive (negative) values of $\rho_{\mathrm{diff}}(z)$ correspond to electron accumulation (depletion) upon carborane adsorption. As expected, $\rho_{\mathrm{diff}}(z)$ integrates to zero. Fig. 3 shows oscillations around zero, which are more pronounced in the Au–S region for both B- and C-bonded carboranes. In particular, electrons are accumulated in the S atoms, while the region close to the Au surface is depleted. This rearrangement is consistent with the changes in Mulliken populations. Upon adsorption, the orbital population of each S atom increases by $\sim$0.1 e, while those of contact Au or B (C) atoms decrease by $\sim$0.03 e for B-bonded (C-bonded) junctions. An interface dipole pointing towards the metal is formed as a consequence of this charge rearrangement. Numerical calculations of the dipole resulting from these $\rho_{\mathrm{diff}}(z)$ profiles yield substantial values. For the B-bonded and C-bonded interfaces, these dipoles are -2.3 D and -2.5 D, respectively. As we discuss below, these contributions arising from charge rearrangement have a significant effect on the total dipole at the interface. However, from Fig. 2 we can see that the most important shift

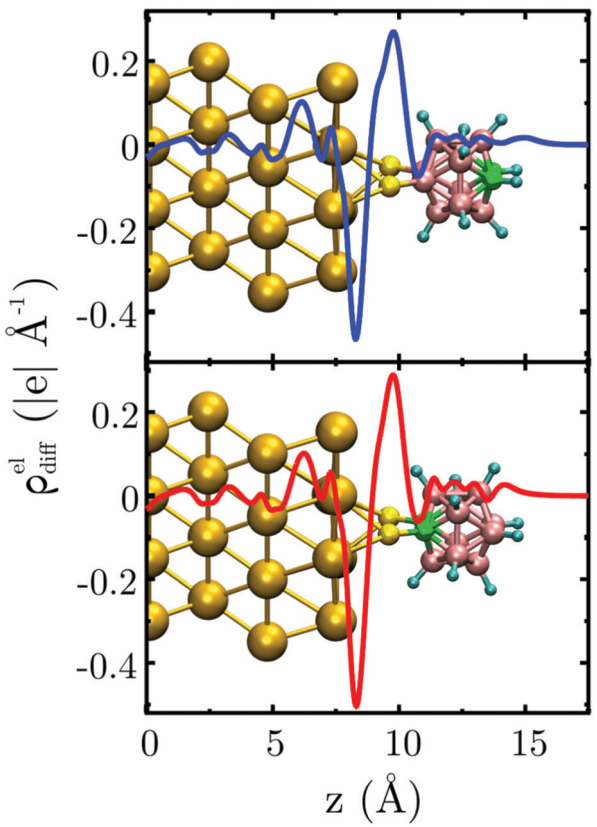

Fig. 3 Plane-averaged electron density difference profiles for B-bonded (top panel, blue) and C-bonded (bottom panel, red) carboranes upon adsorption on the Au(111) surface.

in the work function takes place inside the carborane cage, consistent with the large internal dipole.

Density of states

The spectral properties of the dithiolcarboranes thus adsorbed at the junction exhibit interesting characteristics. The full lines in Fig. 4 show the Projected Density of States (PDOS)[34,45] of carboranedithiols adsorbed vertically on the Au(111) surface, calculated the geometry of Fig. 2 and 3. The PDOS of B-bonded (C-bonded) are shown in blue (red). The different vertical panels show projections onto all molecular atoms, or onto the different chemical species. Dashed lines denote the position of molecular orbitals of the carborane unit cleaved off the Au substrate (while keeping the geometry unchanged). The large shifts between the positions of these states and peaks in the PDOS are consistent with the charge rearrangement at the interface.

From the calculated spectra, for both isomers the occupied state closest to the Fermi level has a strong contribution of the S linker atoms. In the empty part of the spectrum there are differences in the character of the Lowest Unoccupied Molecular Orbital (LUMO) depending on the carborane isomer. The LUMO of the B-functionalized molecule (blue) has a significant contribution of B states. However, in the LUMO of the C-bonded isomer (red), the involvement of B-derived states is lower, and instead it has a stronger C character.

Carborane tilt angle and effect of surface asperities

So far we have discussed the interface properties of carboranes adsorbed vertically on Au. These vertical geometries are local minima in the geometry relaxations but other stable junction geometries are found when the carborane molecule is tilted around the axis connecting both S atoms.

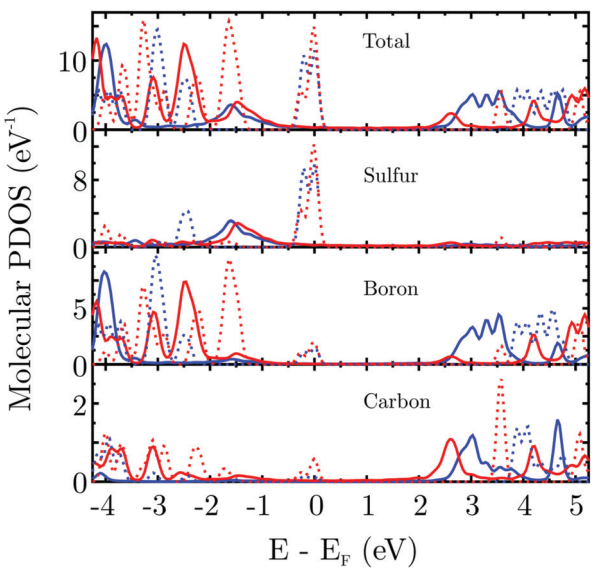

Fig. 4 Calculated molecular PDOS at the interface of B-bonded (blue) and C-bonded (red) carboranes. Dashed lines correspond to the isolated case, obtained by removing all Au atoms while keeping the molecular geometry unchanged.

Since slab calculations involve periodic boundary conditions in the x and y directions, the junction energetics are affected by the electrostatic interaction between the dipole of the unit cell and that of the replicas. Because of this, a vertical orientation of the carborane molecule (with its dipole pointing along the z direction) is unfavourable energetically from purely dipole–dipole considerations. Together with the replicas, this vertical geometry represents a two-dimensional arrangement of parallel dipoles, which is not favourable from an energy standpoint. Instead, the energy of this array of dipoles would be minimized in a horizontal orientation of the molecule, with the inherent carborane dipole parallel to the Au surface. This SAM geometry, with molecules physisorbed above the metal surface, was recently considered in a computational study of carboranethiols.[46] In our work, however, we tilt the molecules around the axis connecting both S atoms, and the carborane molecules remain anchored to the Au surface through the metal–thiolate bonds.

Intuitively, as the tilt angle is increased from a vertical orientation, one can expect the energy to decrease at first due to dipole–dipole interactions. Eventually, for high enough angles, the Au atoms will repel the carborane cage when it comes too close to the metal surface. Within this range, the polar angle leading to the energy minimum will be found. This overall picture is confirmed by atomistic simulations, although with two important caveats. First, simulations showed that this polar tilt angle is a rather soft degree of freedom: there are stable configurations with tilt angles between $\theta \sim 40$ to $\sim$60 degrees within $\sim$200 meV of each other. Second, the tilting of dithiocarboranes was accompanied in many cases with significant deformation of the Au surface layer. For large tilt angles, Au surface atoms bonded to the S linker atoms were pulled out of the surface layer during geometry relaxation. As we discuss below, these distortions of the Au layer strongly affect the total energy and the dipole of the junction.

The calculated dipole and total energy for the B- and C-bonded carboranes are summarized in Fig. 5. Each point corresponds to a relaxed structure obtained in the sampling of azimuthal and polar angles. The value of the polar tilt angle after geometry optimization is shown in the horizontal axis. The vertical axis indicates the total energy, with respect to the lowest value for each (B- or C-bonded) set. The change in the junction dipole with respect to that of the clean Au slab is given by the color bar. Each panel contains $\sim$100 data points.

The results of Fig. 5 show that junctions where the carborane is adsorbed more or less vertically ($\theta < 20$ degrees) are energetically more costly than those with larger tilt angles. As we now discuss, in this latter case, Au atoms are extracted from the metal surface layer. The effect of the adsorbed carborane on the dipole of the junction, shown in the color scale, follows the expected behaviour as a function of tilt (polar) angle: it decreases with increasing tilt angle since the projection onto the vertical direction is smaller. Moreover, since the orientation of the intrinsic dipole is opposite for B- and C-functionalized carboranes, their contributions to the total dipole of the junction as a function of tilt angle go in opposite directions.[47]

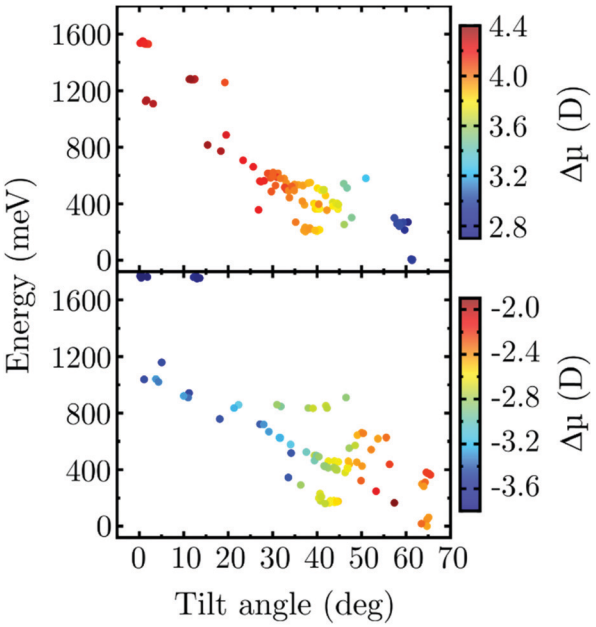

Fig. 5 Energy and change in the slab dipole (color scale) as a function of the final molecular tilt angle for a series of B-bonded (top panel) and C-bonded (bottom panel) carboranes adsorbed on Au(111).

In B-bonded carboranes the intrinsic molecular dipole points upwards, opposite the direction of the Au slab dipole, while for C-bonded molecules both dipoles point towards $-z$. Thus, as the molecular tilt angle θ increases in Fig. 5, the z projection of the carborane dipole decreases in absolute value, and the total dipole of the junction is less positive for B-bonded junctions (top panel) or less negative in the case of C-bonded molecules (bottom panel).

We now comment on the extraction of Au surface atoms due to interaction with the carborane thiolate groups. As mentioned above, we observed this in many simulations, especially for high tilt angles. It is well known that thiolate groups interact strongly with Au and can induce important structural changes in the Au surface.[48,49] Our simulations show instances where one, two and even three Au atoms bonded to molecular S groups were lifted during geometry relaxations by $\sim$1.0 Å or more above the metal surface. These atomic rearrangements stabilize the junction, resulting in a lowering of the total energy. Concurrently, regardless of the adsorbed carborane isomer, this Au rearrangement always contributes positively to the Au slab dipole, which is made less negative. As before, this effect can add to or be cancelled by the inherent dipole of the adsorbed carborane depending on its direction.

To further investigate the role on the interfacial properties of Au structures adsorbed on top of the surface layer, we consider junctions where the carborane isomers are bonded to Au adatoms adsorbed on hollow surface sites. We studied junctions with either a single adatom or three adatoms. Initial geometries were generated by placing the carborane molecules partially mounted on top of the Au adatom(s). One of the S atoms, at a higher distance from the surface, was placed above the Au adsorbate, while the other S atom was positioned closer to the surface. Initial structures were generated having the azimuthal angle span 120 degrees. Although the molecule was initially vertical, it tilted markedly during geometry optimization. Simulations showed no differences between Au adatoms placed on hcp or fcc hollow sites.

These interface calculations with Au adsorbates (see ESI† for details) are in line with the findings on the bare surface. Tilting of carborane molecules during geometry relaxation is accompanied by displacement of adjacent Au atoms and a lowering of the total energy. As on the clean Au surface, interface geometry is controlled by Au–S interactions. Simulations show that the S atom closest to the surface will tend to adsorb close to a hollow site, as expected. However, for the other S atom, initially placed above the adsorbed Au adatom or trimer structure, we found several stable binding geometries. The coordination of this S atom strongly influences the total energy of the junction. Regardless of whether the Au adsorbates consisted of one or three adatoms, the structures with the lowest energy had the S atom bonded to two Au atoms in a bridge-like configuration. Whenever the S atom was bonded to one Au atom only, the energy was significantly higher. Due to steric repulsion with the carborane cage, no geometries were found where the S atom was bonded on a hollow site above the Au trimer.

These calculations of carboranes bonded to Au adsorbates corroborate the picture of strong Au–S interaction and saturation of the S orbitals governing the interface energetics and in inducing substantial changes in the atomistic structure of the Au surface.

4 Conclusions

In summary, we investigated the structural and interface electronic properties of carboranedithiols adsorbed on Au(111). We considered two carborane positional isomers for which the intrinsic molecular dipole points towards the surface or away from it. We sampled a large number of interface geometries exploring a wide range of carborane orientations. We found that adsorption of carborane molecules results in considerable changes in the gold work function. When the carborane is functionalized through B atoms, the molecular dipole points towards the vacuum and the work function is significantly reduced. On the other hand, the intrinsic dipole of C-functionalized carborane points towards the Au surface and the work function is increased. We find that the range of work function changes resulting from carborane adsorption can be of the order of 1 eV. We characterized the electronic structure at the interface, and analyzed the changes in electron density upon adsorption. Our results showed that charge rearrangement at the interface mostly involves the Au–S covalent bonds.

From the large number of structures considered, we saw that the strong metal–thiolate bonds were the main driving mechanism determining the metal–molecule geometry. In particular, coordination of the S bonds led in many cases to the tilting of the adsorbed carborane and to the rearrangement of Au atoms. On the clean Au(111) surface, this tilting was related to

Au atoms being lifted from the surface layer. On surfaces which had one or three Au adatoms, these structures were bonded to one of the molecular thiolate linker groups, often also involving Au atoms extracted from the surface.

Simulations showed that the lifting of Au atoms lowered the total energy, stabilizing the junction configuration. These changes in the atomistic structure of the interface have important consequences for the junction energy and electronic properties. First, they are associated with changes in the molecular geometry, particularly in the tilting of the carborane cage. This alters the component of the molecular dipole perpendicular to the surface and has a clear impact on the potential drop across the interface and work function modification. Second, displacement of Au atoms alters the properties of the metal slab, reducing the magnitude of its dipole. The large intrinsic dipole of the carborane structure has the strongest influence on interface electronic properties, in particular, the work function can be modified upon adsorption by $\sim$1 eV on either the direction depending on molecular orientation. However, simulations also showed that the junction electronic structure depends sensitively on the details of the metal–carborane interface, and in particular on the surface roughness at the atomistic level, which may impact the properties of ultra-thin metal–organic interfaces and films.

Our work thus highlights the importance of accurately describing the atomistic structure at the interface and illustrates how the adsorption of carboranes can be used to modify the interface electronic properties and to tune the metal work function.

Conflicts of interest

There are no conflicts to declare.

Acknowledgements

We gratefully acknowledge financial support from project TH02020628 of the Technological Agency of the Czech Republic, project 17-27338Y of the Czech Science Foundation, the Purkyně Fellowship program of the Czech Academy of Sciences, and the Operational Programme ''Research, Development and Education'' financed by European Structural and Investment Funds and the Czech Ministry of Education, Youth and Sports (Project No. SOLID21 – CZ.02.1.01/0.0/0.0/16_019/0000760). Computational resources were provided by the National Grid Infrastructure MetaCentrum and the ''Projects of Large Research, Development, and Innovations Infrastructures'' program (CESNET LM2015042 and LM2015087).

References

1 J. Kim, Y. S. Rim, Y. Liu, A. C. Serino, J. C. Thomas, H. Chen, Y. Yang and P. S. Weiss, Interface Control in Organic Electronics Using Mixed Monolayers of Carboranethiol Isomers, *Nano Lett.*, 2014, **14**, 2946–2951.

2 R. K. Smith, P. A. Lewis and P. S. Weiss, Patterning self-assembled monolayers, *Prog. Surf. Sci.*, 2004, **75**, 1–68.

3 J. C. Love, L. A. Estroff, J. K. Kriebel, R. G. Nuzzo and G. M. Whitesides, Self-Assembled Monolayers of Thiolates on Metals as a Form of Nanotechnology, *Chem. Rev.*, 2005, **105**, 1103–1170.

4 C. Vericat, M. E. Vela, G. Benitez, P. Carro and R. C. Salvarezza, Self-assembled monolayers of thiols and dithiols on gold: new challenges for a well-known system, *Chem. Soc. Rev.*, 2010, **39**, 1805–1834.

5 J. J. Gooding and S. Ciampi, The molecular level modification of surfaces: from self-assembled monolayers to complex molecular assemblies, *Chem. Soc. Rev.*, 2011, **40**, 2704–2718.

6 F. Flores, J. Ortega and H. Vázquez, Modelling energy level alignment at organic interfaces and density functional theory, *Phys. Chem. Chem. Phys.*, 2009, **11**, 8658–8675.

7 D. A. Wann, P. D. Lane, H. E. Robertson, T. Baše and D. Hnyk, The gaseous structure of *closo*-9,12-(SH)2-1,2-$C_2B_{10}H_{10}$, a modifier of gold surfaces, as determined using electron diffraction and computational methods, *Dalton Trans.*, 2013, **42**, 12015–12019.

8 F. von Wrochem, F. Scholz, D. Gao, H.-G. Nothofer, A. Yasuda, J. M. Wessels, S. Roy, X. Chen and J. Michl, High-Band-Gap Polycrystalline Monolayers of a 12-Vertex *p*-Carborane on Au(111), *J. Phys. Chem. Lett.*, 2010, **1**, 3471–3477.

9 R. N. Grimes, Carboranes in the chemist's toolbox, *Dalton Trans.*, 2015, **44**, 5939–5956.

10 S. Fujii, U. Akiba and M. Fujihira, Geometry for Self-Assembling of Spherical Hydrocarbon Cages with Methane Thiolates on Au(111), *J. Am. Chem. Soc.*, 2002, **124**, 13629–13635.

11 T. Baše, Z. Bastl, Z. Plzák, T. Grygar, J. Plešek, M. J. Carr, V. Malina, J. Šubrt, J. Boháček, E. Večerníková and O. Kříž, Carboranethiol-Modified Gold Surfaces. A Study and Comparison of Modified Cluster and Flat Surfaces, *Langmuir*, 2005, **21**, 7776–7785.

12 S. Balaz, A. N. Caruso, N. P. Platt, D. I. Dimov, N. M. Boag, J. I. Brand, Y. B. Losovyj and P. A. Dowben, The Influence of the Molecular Dipole on the Electronic Structure of Isomeric Icosahedral Dicarbadodecaborane and Phosphacarbadodecaborane Molecular Films, *J. Phys. Chem. B*, 2007, **111**, 7009–7016.

13 S. A. Claridge, W.-S. Liao, J. C. Thomas, Y. Zhao, H. Cao, S. Cheunkar, A. C. Serino, A. M. Andrews and P. S. Weiss, From the Bottom Up: Dimensional Control and Characterization in Molecular Monolayers, *Chem. Soc. Rev.*, 2013, **42**, 2725–2745.

14 F. Scholz, H.-G. Nothofer, J. M. Wessels, G. Nelles, F. von Wrochem, S. Roy, X. Chen and J. Michl, Permethylated 12-Vertex *p*-Carborane Self-Assembled Monolayers, *J. Phys. Chem. C*, 2011, **115**, 22998–23007.

15 L. J. Yeager, F. Saeki, K. Shelly, M. F. Hawthorne and R. L. Garrell, A New Class of Self-Assembled Monolayers:

closo-$B_{12}H_{11}S^{3-}$ on Gold, *J. Am. Chem. Soc.*, 1998, **120**, 9961–9962.
16 H. Beall, in *Boron Hydride Chemistry*, ed. E. L. Muetterties, Academic Press, 1975, pp. 301–347.
17 R. N. Grimes, *Carboranes*, Academic Press, Oxford, 2nd edn, 2011, pp. 301–540.
18 G.-X. Jin, Advances in the chemistry of organometallic complexes with 1,2-dichalcogenolato-*o*-carborane ligands, *Coord. Chem. Rev.*, 2004, **248**, 587–602.
19 A. M. Spokoyny, C. W. Machan, D. J. Clingerman, M. S. Rosen, M. J. Wiester, R. D. Kennedy, C. L. Stern, A. A. Sarjeant and C. A. Mirkin, A coordination chemistry dichotomy for icosahedral carborane-based ligands, *Nat. Chem.*, 2011, **3**, 590–596.
20 P. Matějíček, M. Uchman, M. Lepšík, M. Srnec, J. Zedník, P. Kozlík and K. Kalíková, Preparation and Separation of Telechelic Carborane-Containing Poly(ethylene glycol)s, *ChemPlusChem*, 2013, **78**, 528–535.
21 R. G. Nuzzo and D. L. Allara, Adsorption of bifunctional organic disulfides on gold surfaces, *J. Am. Chem. Soc.*, 1983, **105**, 4481–4483.
22 H. Grönbeck, A. Curioni and W. Andreoni, Thiols and Disulfides on the Au(111) Surface: The Headgroup–Gold Interaction, *J. Am. Chem. Soc.*, 2000, **122**, 3839–3842.
23 D. L. Kokkin, R. Zhang, T. C. Steimle, I. A. Wyse, B. W. Pearlman and T. D. Varberg, Au–S Bonding Revealed from the Characterization of Diatomic Gold Sulfide, AuS, *J. Phys. Chem. A*, 2015, **119**, 11659–11667.
24 A. Ulman, Formation and Structure of Self-Assembled Monolayers, *Chem. Rev.*, 1996, **96**, 1533–1554.
25 J. N. Hohman, S. A. Claridge, M. Kim and P. S. Weiss, Cage molecules for self-assembly, *Mater. Sci. Eng., R*, 2010, **70**, 188–208.
26 J. N. Hohman, P. Zhang, E. I. Morin, P. Han, M. Kim, A. R. Kurland, P. D. McClanahan, V. P. Balema and P. S. Weiss, Self-Assembly of Carboranethiol Isomers on Au{111}: Intermolecular Interactions Determined by Molecular Dipole Orientations, *ACS Nano*, 2009, **3**, 527–536.
27 E. C. M. Ting, T. Popa and I. Paci, Surface-site reactivity in small-molecule adsorption: A theoretical study of thiol binding on multi-coordinated gold clusters, *Beilstein J. Nanotechnol.*, 2016, **7**, 53–61.
28 Y. Xue, X. Li, H. Li and W. Zhang, Quantifying thiol–gold interactions towards the efficient strength control, *Nat. Commun.*, 2014, **5**, 4348.
29 J. K. Bhattarai, D. Neupane, V. Mikhaylov, A. V. Demchenko and K. J. Stine, in *Carbohydrate*, ed. M. Caliskan, I. H. Kavakli and G. C. Oz, InTech, 2017.
30 D. C. Kennedy, D. R. Duguay, L.-L. Tay, D. S. Richeson and J. P. Pezacki, SERS detection and boron delivery to cancer cells using carborane labelled nanoparticles, *Chem. Commun.*, 2009, 6750–6752.
31 A. M. Cioran, A. D. Musteti, F. Teixidor, Ž. Krpetić, I. A. Prior, Q. He, C. J. Kiely, M. Brust and C. Viñas, Mercaptocarborane-Capped Gold Nanoparticles: Electron Pools and Ion Traps with Switchable Hydrophilicity, *J. Am. Chem. Soc.*, 2012, **134**, 212–221.
32 J. C. Thomas, D. P. Goronzy, A. C. Serino, H. S. Auluck, O. R. Irving, E. Jimenez-Izal, J. M. Deirmenjian, J. Macháček, P. Sautet, A. N. Alexandrova, T. Baše and P. S. Weiss, Acid–Base Control of Valency within Carboranedithiol Self-Assembled Monolayers: Molecules Do the Can-Can, *ACS Nano*, 2018, **12**, 2211–2221.
33 V. I. Bregadze, Dicarba-*closo*-dodecaboranes $C_2B_{10}H_{12}$ and their derivatives, *Chem. Rev.*, 1992, **92**, 209–223.
34 J. M. Soler, E. Artacho, J. D. Gale, A. García, J. Junquera, P. Ordejón and D. Sánchez-Portal, The SIESTA method for *ab initio* order-*N* materials simulation, *J. Phys.: Condens. Matter*, 2002, **14**, 2745–2779.
35 M. Dion, H. Rydberg, E. Schröder, D. C. Langreth and B. I. Lundqvist, van der Waals Density Functional for General Geometries, *Phys. Rev. Lett.*, 2004, **92**, 246401.
36 G. Román-Pérez and J. M. Soler, Efficient Implementation of a van der Waals Density Functional: Application to Double-Wall Carbon Nanotubes, *Phys. Rev. Lett.*, 2009, **103**, 096102.
37 G. Heimel, L. Romaner, E. Zojer and J.-L. Bredas, The Interface Energetics of Self-Assembled Monolayers on Metals, *Acc. Chem. Res.*, 2008, **41**, 721–729.
38 D. Cahen and A. Kahn, Electron Energetics at Surfaces and Interfaces: Concepts and Experiments, *Adv. Mater.*, 2003, **15**, 271–277.
39 G. Foti and H. Vázquez, Tip-induced gating of molecular levels in carbene-based junctions, *Nanotechnology*, 2016, **27**, 125702.
40 J. Junquera, M. Zimmer, P. Ordejón and P. Ghosez, First-principles calculation of the band offset at $BaO/BaTiO_3$ and $SrO/SrTiO_3$ interfaces, *Phys. Rev. B: Condens. Matter Mater. Phys.*, 2003, **67**, 155327.
41 A. Vetushka, L. Bernard, O. Guseva, Z. Bastl, J. Plocek, I. Tomandl, A. Fejfar, T. Baše and P. Schmutz, Adsorption of oriented carborane dipoles on a silver surface, *Phys. Status Solidi B*, 2016, **253**, 591–600.
42 T. Baše, Z. Bastl, M. Šlouf, M. Klementová, J. Šubrt, A. Vetushka, M. Ledinský, A. Fejfar, J. Macháček, M. J. Carr and M. G. S. Londesborough, Gold Micrometer Crystals Modified with Carboranethiol Derivatives, *J. Phys. Chem. C*, 2008, **112**, 14446–14455.
43 V. Obersteiner, D. A. Egger and E. Zojer, Impact of Anchoring Groups on Ballistic Transport: Single Molecule *vs.* Monolayer Junctions, *J. Phys. Chem. C*, 2015, **119**, 21198–21208.
44 G. Heimel, L. Romaner, E. Zojer and J.-L. Brédas, Toward Control of the Metal–Organic Interfacial Electronic Structure in Molecular Electronics: A First-Principles Study on Self-Assembled Monolayers of π-Conjugated Molecules on Noble Metals, *Nano Lett.*, 2007, **7**, 932–940.
45 D. S. Sholl and J. A. Steckel, *Density functional theory: a practical introduction*, Jonh Wiley & Sons, Hoboken (New Jersey), 2009.
46 E. Mete, A. Yılmaz and M. F. Danışman, A van der Waals density functional investigation of carboranethiol self-assembled monolayers on Au(111), *Phys. Chem. Chem. Phys.*, 2016, **18**, 12920–12927.

47 J. Chen, S. Gathiaka, Z. Wang and M. Thuo, Role of Molecular Dipoles in Charge Transport across Large Area Molecular Junctions Delineated Using Isomorphic Self-Assembled Monolayers, *J. Phys. Chem. C*, 2017, **121**, 23931–23938.

48 D. Krüger, H. Fuchs, R. Rousseau, D. Marx and M. Parrinello, Pulling Monatomic Gold Wires with Single Molecules: An Ab Initio Simulation, *Phys. Rev. Lett.*, 2002, **89**, 186402.

49 R. Mazzarello, A. Cossaro, A. Verdini, R. Rousseau, L. Casalis, M. F. Danisman, L. Floreano, S. Scandolo, A. Morgante and G. Scoles, Structure of a CH3 Monolayer on Au(111) Solved by the Interplay between Molecular Dynamics Calculations and Diffraction Measurements, *Phys. Rev. Lett.*, 2007, **98**, 016102.